Geophysical Research Letters

RESEARCH LETTER
10.1029/2023GL106298

Quantifying ENSOs Impact on Australia's Regional Monthly Rainfall Risk

Shayne McGregor[1,2], **Ailie Gallant**[1,2], **and Peter van Rensch**[1,2]

[1]School of Earth Atmosphere and Environment, Monash University, Monash University, VIC, Australia, [2]Centre of Excellence for Climate Extremes, Monash University, Monash University, VIC, Australia

Key Points:

- We adapt the commonly used Fraction of Attributable Risk method to attribute rainfall variability to the El Niño-Southern Oscillation
- We present the ENSO induced change in risk and the FAR for all observed spring rainfall rates for three eastern Australian regions
- The increased spring 2022 East Australian rainfall was >5 times more likely, and largely attributed to the La Niña conditions present

Supporting Information:

Supporting Information may be found in the online version of this article.

Correspondence to:

S. McGregor,
shayne.mcgregor@monash.edu

Citation:

McGregor, S., Gallant, A., & van Rensch, P. (2024). Quantifying ENSOs impact on Australia's regional monthly rainfall risk. *Geophysical Research Letters*, *51*, e2023GL106298. https://doi.org/10.1029/2023GL106298

Received 7 SEP 2023
Accepted 28 FEB 2024

Abstract The El Niño-Southern Oscillation (ENSO) is considered an important driver of rainfall variability in Australia, amongst many other global locations. Despite knowledge of the expected modulation of seasonal rainfall by ENSO, there is no consistently used method to quantify the role that specific ENSO events play in driving the observed anomalous rainfall. In this manuscript we adapt the Fraction of Attributable Risk (FAR) method, commonly used to identify the anthropogenic impact on a particular event, to quantify the impact of ENSO on the occurrence of monthly rainfall anomalies. We also explicitly calculate the ENSO induced change in risk and the FAR for all observed spring rainfall rates for our eastern Australian regions. A prominent role for ENSO in driving the large spring 2022 rainfall anomalies is identified. Though we choose to focus on ENSOs impact on rainfall in various Eastern Australian regions, the results are applicable to other climate modes, regions and climatic variables.

Plain Language Summary The El Niño-Southern Oscillation (ENSO) is considered an important driver of rainfall variability in Australia, amongst many other global locations. Despite understanding how ENSO is expected to alter rainfall, we do not currently quantify the role ENSO played in driving a observed rainfall anomaly in any given season. In this manuscript we adapt a method that is commonly used to identify the anthropogenic impact on a particular event; and instead, we quantify the impact of ENSO on the occurrence of monthly rainfall anomalies. We then calculate the ENSO-induced change in risk for all observed spring rainfall rates for our selected eastern Australian regions. A prominent role for ENSO in driving large rainfall anomalies of spring 2022 is also identified. Though we choose to focus on ENSOs impact on rainfall in various eastern Australian regions in this study, the results are applicable to other climate modes, regions and climatic variables.

1. Introduction

The El Niño-Southern Oscillation (ENSO) has been identified in the literature as being important in driving rainfall variability in Australia (King et al., 2013; Power et al., 1999), amongst many other global locations (Taschetto et al., 2020). ENSO is characterized by sea surface temperature anomalies (SSTA) over multiple months in the central/eastern equatorial Pacific which are accompanied by large scale changes in rainfall and atmospheric circulation. For instance, a SSTA cooling in this region (i.e., a La Niña event) is often accompanied by an increase in easterly trade winds and rainfall in the western tropical Pacific, while a SSTA warming in this region (i.e., an El Niño event) is often accompanied by weakening of the easterly trade winds and an eastward shift in equatorial rainfall (Timmermann et al., 2018).

The Eastern Australian regional rainfall impact of ENSO, which has been widely reported (McBride & Nicholls, 1983) is strongest on September–November (SON) rainfall (Figure 1a). For instance, given La Niña conditions in the Pacific, during SON much of eastern Australia would be expecting more rainfall than normal in the monthly mean and extreme rainfall sense (Hendon et al., 2014; King et al., 2013; Nicholls, 1988; Risbey et al., 2009), along with a higher chanced of flooding (Kiem et al., 2003). During El Niño events on the other hand, much of eastern Australia would be expecting dryer than normal conditions and less extreme rainfall and a higher chance of drought (Van Dijk et al., 2013). These rainfall impacts of ENSO also lead to associated impacts on river flow and crop yields in many eastern Australian areas (Chiew et al., 1998; Nicholls, 1997; Power et al., 1999).

Research has also highlighted that the impact of ENSO on Australian rainfall in not symmetric (Cai et al., 2010; King et al., 2013; Power & Colman, 2006; Power et al., 2006). Rather, La Niña events tend to have a larger impact than El Niño events on eastern Australian rainfall. The general rule of thumb is that

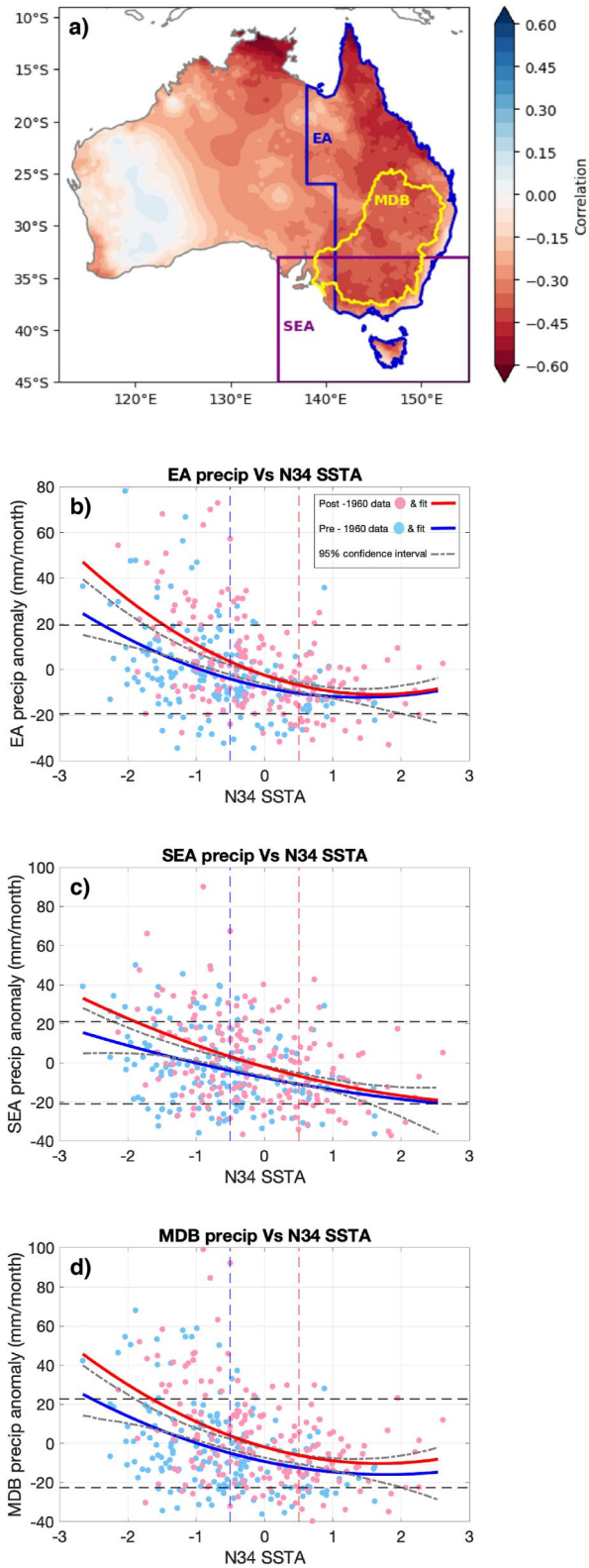

Figure 1.

the increase in rainfall expected during La Niña is linearly related to the magnitude of the event, while the magnitude of an El Niño is only weakly related to how dry conditions will become (Figure 1b). Research also suggests that these ENSO teleconnections display changes on inter-annual, decadal and longer time scales (King et al., 2013; Power et al., 1999). However, it is currently unclear whether this modulation is distinct from Australia's nonlinear rainfall to ENSO events (Power et al., 2006). Recent studies also suggest that the anthropogenically induced SST warming has acted to enhance the rainfall impacts of recent La Niña events (Ummenhofer et al., 2015).

Despite our knowledge of expected ENSO modulation of seasonal rainfall, we currently do not seek to quantify the change in risk of anomalous Australian regional average rainfall due to ENSO or any other mode of climate variability. However, this is something that is commonly done to identify the impact of anthropogenic climate change on a particular event utilizing the Fraction of Attributable Risk (FAR) framework (Allen, 2003; Karoly et al., 2016; Stott et al., 2004). For instance, several studies utilized this framework to investigate an anthropogenic influence on Australian extreme rainfall (Hope et al., 2018; King, 2018; King et al., 2013).

In this manuscript, we adapt the FAR method to quantify the impact of ENSO on the occurrence of anomalous monthly mean rainfall in various Eastern Australian regions. We focus on utilizing observational data to sidestep any perceived issues around the model representation of ENSO and its Australian teleconnections (C. Chung et al., 2023; Planton et al., 2020). That is, we seek to estimate the change in risk of an observed rainfall monthly rainfall anomaly of magnitude X or greater occurring given the phase of ENSO.

This paper is organized as follows. In Section 2 we present the data utilized in this study along with details of how we intend to use the FAR framework to attribute observed rainfall changes to ENSO. The change in risk of monthly rainfall anomalies for select Australian regions of differing sizes are then presented in Section 3, while Section 4 presents a case study of East Australian regional rainfall during the 2022 La Nina event. Section 5 discusses some apparent rainfall changes and their possible relationship to anthropogenic climate change. Discussion and conclusions are presented in Section 6.

2. Data and Methods

2.1. Climate Mode Indices

To calculate our climate mode indices we use observational SST estimates from the National Oceanic and Atmospheric Administration Extended Reconstruction SST, version 5 (ERSST v5) product (Huang et al., 2017) consisting of monthly mean values from 1854 to the present on a 2° × 2° horizontal grid globally. ENSO is represented by area averaged SSTA in the N34 region (170°W–120°W & 5°S–5°N). As we are focusing on the September–October (SON) season when ENSO is reported to have its strongest impacts on Australian rainfall, we only utilize the monthly anomalous data during SON.

Here we utilize the NOAA SSTA threshold for the definition of ENSO events without considering their time criteria. Rather, El Niño is defined when monthly mean SSTA are above the 0.5°C threshold, while a SSTA below the

−0.5°C threshold is defined as La Niña (Figures 1b–1d). Analysis of Figure 1 also suggests that this SSTA threshold is appropriate for the rainfall impacts of ENSO events.

2.2. Rainfall Data

Rainfall for SON was sourced from the Bureau of Meteorology's Australian Gridded Climate Data (AGCD) for the period 1900–2022 (A. Evans et al., 2020). Regional average rainfall was utilized for three regions, Eastern Australia (EA; Queensland, New South Wales, Victoria and Tasmania), SouthEastern Australia (SEA; south of 33°S, east of 135°E) and the Murray–Darling catchment (MDB) (Figure 1a). It is noted that linearly detrending the data has little impact on the broad results presented here.

The EA region, which covers a vast area, was selected to maximize the signal to noise ratio of the rainfall impacts of ENSO events. The two other regions utilized in this study, SEA and MDB which are both largely contained with the EA region, are utilized to explore if robust ENSO impacts can also be identified in smaller regions.

2.3. Fraction of Attributable Risk (FAR) and Risk Ratio (RR) Description

The FAR framework is often used to attribute some observed event to anthropogenic climate change. In this case, once an event is identified in the observations and the climate model/s of choice are deemed to realistically represent this variable in the region of interest, there are three main steps required for attribution (King et al., 2016). Firstly, the probability of an event of this magnitude is calculated (P_0) in the absence of anthropogenic climate change (CMIP defined pre-Industrial control simulations), then the probability of that same event is calculated (P_1) with the impact of anthropogenic climate change included (CMIP defined historical simulations). Then the Fraction of Attributable Risk (FAR) is then identified by the equation:

$$\mathrm{FAR} = 1 - P_0/P_1 \tag{1}$$

A FAR of 1 suggests that the given event would not have occurred in the absence of anthropogenic forcing, while a FAR of 0.5 suggests that 50% of events that occurred of this magnitude or greater can be attributed to the forcing (Stott et al., 2004). We also utilize the Risk Ratio, which is defined be the equation:

$$\mathrm{RR} = P_1/P_0 \tag{2}$$

Where a Risk Ratio of greater than 1 indicates an increase in risk due to anthropogenic forcing, while a Risk Ratio of less than 1 indicates a decrease in the risk. The risk ratio is not defined if the P_0 has a probability of 0.

In our study, however, we are instead trying to estimate the change in risk of a rainfall event of magnitude X or greater occurring given the phase of ENSO using only observations, not models. To differentiate what we are doing here from the traditional use of FAR analysis for anthropogenic climate change attribution we will attach a subscript to the FAR acronym to identify the climate mode and phase of interest. When calculating FAR for El Niño events ($\mathrm{FAR_{EN}}$) or La Niña events ($\mathrm{FAR_{LN}}$), the P_1 is the probability of a certain rainfall event during El Niño and La Niña months, respectively (Figures 1b–1d). The P_0 in both cases would simply be the probability of the event occurring during those months where ENSO is considered to be neutral (i.e., between ±0.5°C).

Probabilities of event occurrences are calculated using the Kaplan-Meier estimate of the cumulative distribution function (CDF) within Matlab, which is also known as the empirical CDF [i.e., within the Matlab "ecdf" routine the default "cdf" function was utilized and no data were censored]. We utilize the observational data in the 73 year period between 1950 and 2022 for our main calculation, as it is deemed to be the most robustly observed. Details of the 95% confidence intervals utilized for the CDFs can be found in Supporting Information S1.

Figure 1. ENSO and Australian SON rainfall relationship. (a) Correlation coefficients calculated between ENSO (represented by area averaged SSTA in the N34 region; 170°W–120°W & 5°S–5°N) in SON and the SON grid point level average rainfall anomalies (1900–2022). Overlaying are the outlines of the Eastern Australian (EA), South Eastern Australian (SEA) and Murray Darling Basin (MDB). (b–d) Monthly SON regional EA, SEA and MDB anomalous rainfall plotted as a function of SON ENSO. Red dashed vertical lines indicate the SSTA threshold for El Niño events, while blue dashed vertical lines indicate the SSTA threshold for La Niña events. The horizontal black dashed lines represent the ±1 standard deviation of the regional rainfall. Blue markers and fitted line are for data from the pre-1960 period, while red markers and fitted line are for data from the post-1960 period. Dash dot gray lines are 95% confidence bounds on the fitted lines.

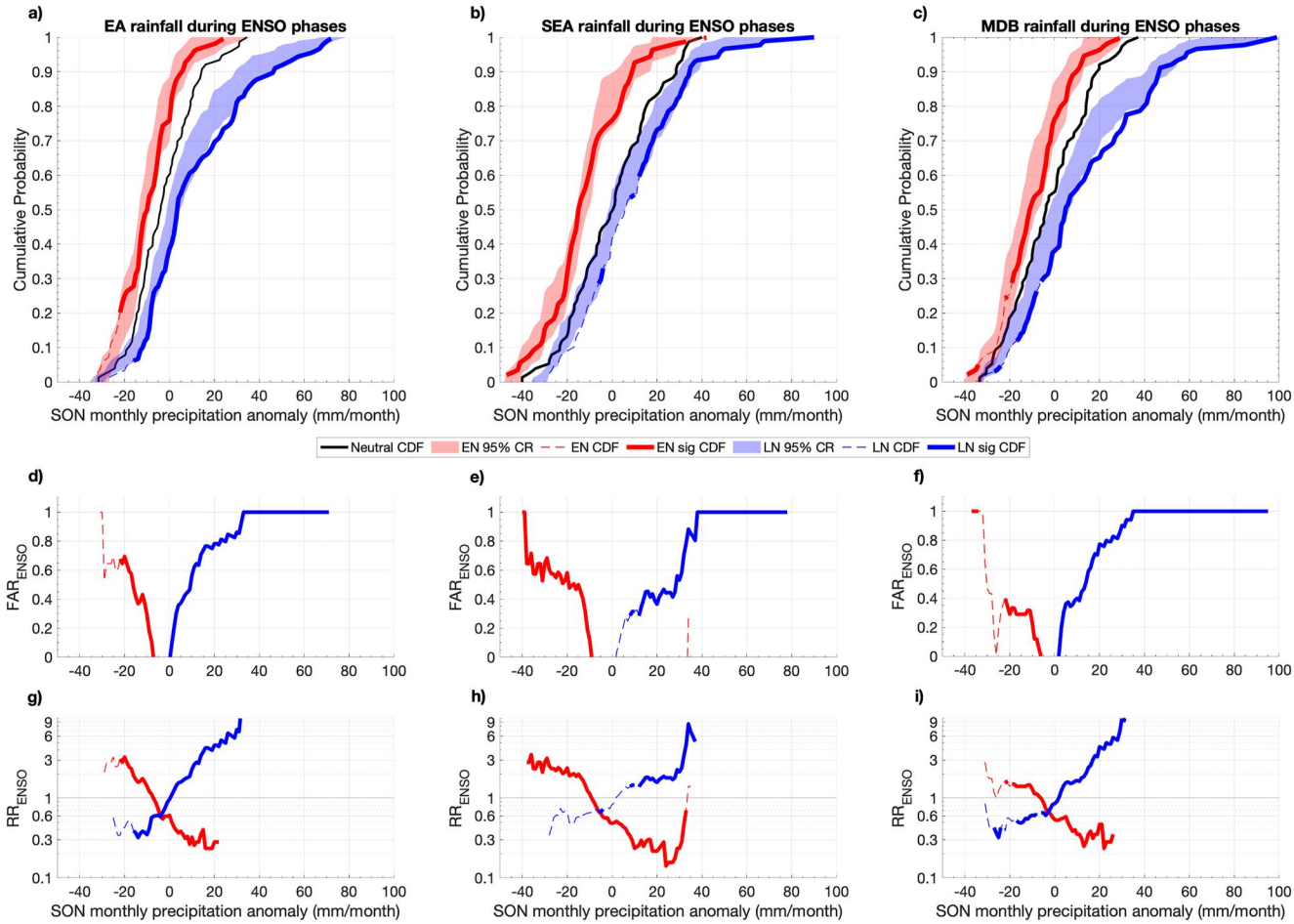

Figure 2. CDFs of Australian regional SON rainfall anomalies during ENSO phases (see legend) is presented in the top row, for (a) East Australia (EA), (b) South East Australia (SEA), and (c) Murray Darling Basin (MDB). The Fraction of Attributable Risk of regional rainfall during ENSO phases (FAR_{ENSO}) is presented in the second row, where EA, SEA, and MDB are presented in (d), (e) and (f), respectively. The Risk Ratio of regional rainfall during ENSO phases (RR_{ENSO}) is then presented the third row, where EA, SEA, and MDB are presented in (g), (h) and (i), respectively. In all panels solid thick blue and red lines respectively indicate that the La Niña and El Niño related changes are statistically significant, while dashed lines indicate that the changes are not significant. Shaded regions in (a)–(c) represent the 95% confidence range estimated from Monte-Carlo sampling (see Supporting Information S1).

3. ENSO Australian Regional Rainfall Impacts

In the following subsections we will discuss the regional CDF shifts for La Niña and El Niño events along with their impacts on the FAR_{ENSO} and RR_{ENSO}, relative to the ENSO neutral phase.

3.1. Eastern Australia

3.1.1. La Niña

Considering the La Niña case for this region (Figure 2a), there is a clear shift of the CDF to wetter values when compared to the neutral case. The significance of this CDF shift is highlighted by the fact that the neutral CDF values fall outside of the La Niña confidence range for the overwhelming majority of rainfall values. The exception here is for extremely low rainfall values, suggesting that large drying can sometimes occur during La Niña events. We also note that the La Niña CDF for the EA region falls outside of its own confidence interval for anomalies between 15 and 30 mm/month, as this is explored further in Section 5.

The role La Niña events have in driving increased EA region rainfall is demonstrated by focusing in on the example rainfall range of between 20 and 30 mm/month. The average risk ratio (RR_{LN}) suggests that rainfall in this range is more than 5.5 times more likely to occur during La Niña events compared to neutral years, while the

FAR_{LN} is roughly 0.81, meaning that on average 81% of observed rainfall events in this range can be attributed to La Niña events.

Also evident from the risk ratio (RR_{LN}) is the decreased probability of anomalously dry conditions occurring during La Nina events. The average RR_{LN} for anomalous EA rainfall of between −5 and −20 mm/month is 0.45, meaning this is drying of this magnitude is on average 55% less likely to occur during La Niña events, when compared to neutral conditions.

3.1.2. El Niño

For the EA region El Niño case (Figure 2a), there is a clear shift of the CDF to dryer values when compared to the neutral case. The neutral CDF values fall outside of the 95% confidence range of the El Niño CDF for the large majority of the CDF, highlighting the statistical significance of this shift to dryer conditions. Again, the only real exception to this is at the very dry end of the El Niño CDF, where the neutral CDF falls within the El Niño CDF 95% confidence interval. This suggests that extremely dry conditions can also occur during neutral years, though not as likely as they are during El Niño events.

The role of El Niño events in driving decreased EA region rainfall is evident looking at FAR_{EN} and RR_{EN} (Figures 2d and 2g). Consider an anomalous EA region drying of between −22 and −15 mm/month, the mean risk ratio (RR_{EN}) suggests that this is 2.6 times more likely to occur during El Niño events compared to neutral years, while the mean FAR_{EN} is roughly 0.59, meaning that 59% of events with this magnitude can be attributed to El Niño events.

On the other hand, the RR_{EN} also indicates that normal to increased rainfall is statistically significantly much less likely during an El Niño event. For instance, near normal rainfall (defined as anomalies between ±5 mm/month) have an average RR_{EN} of 0.52, meaning they are almost 50% less likely to occur in an El Niño event than they are during neutral conditions. Looking at anomalous rainfall increases of 5–20 mm/month, these have an average RR_{EN} of 0.29, meaning they are approximately 69% less likely to occur during El Niño events than they are during neutral conditions.

3.2. South Eastern Australia

3.2.1. La Niña

The CDF shift to wetter values compared to neutral conditions is reduced for the SEA region, relative to the EA region. A similar reduction is also seen in the precipitation scatter plots (Figures 1b and 1c). As such, the neutral CDF is contained within the La Niña CDF 95% confidence levels for the majority of anomalous low and near zero rainfall values (Figure 2b). The CDF shifts for anomalous rainfall amounts above ∼10 mm/month, including high rainfall values (i.e., >38 mm/month) that have not occurred in the observational past in the absence of a La Niña event, are significantly different to neutral years.

The role of La Niña events in driving increased SEA rainfall remains clear looking at FAR_{EN} and RR_{EN} (Figures 2e and 2h). Consider an anomalous SEA region rainfall of between 20 and 30 mm/month, the average risk ratio (RR_{LN}) suggests that anomalous rainfall in this range is roughly 1.8 times more likely to occur during La Niña events compared to neutral years, while the average FAR_{LN} suggests that 45% of rainfall events in this range can be attributed to La Niña events. On the other hand, the decreased risk of anomalously dry conditions during La Niña events is not statistically significant.

3.2.2. El Niño

In contrast to this region's response to La Niña events, which is reduced compared to the EA region, this CDF shift toward dryer values during El Niño years appears to be consistent in magnitude with that of the EA region CDF shift (Figure 2b). The large majority of the neutral CDF values fall outside of the 95% confidence range of the El Niño CDF, highlighting the statistical significance of this shift to dryer conditions. The only real exception to this is at the very wet ends of the El Niño CDF, where the neutral CDF falls within the El Niño CDF 95% confidence interval. This suggests that extreme rainfall at the wet end of the CDF may not be significantly different between El Niño and Neutral years.

The decreased EA region rainfall during El Niño events is evident looking at FAR_{EN} and RR_{EN} (Figures 2e and 2h). Looking at the increased risk of anonymously dry regional rainfall of −38 to −20 mm/month during El Niño years, the mean risk ratio (RR_{EN}) suggests that this is 2.5 times more likely to occur when compared to neutral years. In this situation the mean FAR_{EN} suggests that 60% of events with this magnitude can be attributed to El Niño events.

The RR_{EN} also indicates that normal and increased rainfall is much less likely during an El Niño event. For instance, the RR_{EN} of having normal rainfall (e.g., between ± 5 mm/month) is 0.52, suggesting that normal rainfall in this region is 48% less likely to occur during El Niño events. On the other hand, anomalous rainfall increases of between 5 and 20 mm/month have an average RR_{EN} of 0.29, meaning they are approximately 71% less likely to occur during El Niño events than they are during neutral conditions.

3.3. Murray Darling Basin

3.3.1. La Niña

There is a clear shift of the MDB CDF to wetter values during La Niña events (Figure 2c), which appears to be a similar magnitude to that of the EA region (Figure 2a). The neutral CDF falls outside of the La Niña CDF 95% confidence levels for small to moderate negative rainfall anomalies and all positive rainfall anomalies, while the neutral CDF appears to lie on the edge of this confidence interval for strong negative rainfall anomalies. Again, we note that the La Niña CDF for MDB region lies near the edge of its own confidence interval, even falling outside of this interval for anomalies between 10 and 40 mm/month, as this is explored further in Section 5.

The likelihood of increased SEA rainfall during La Niña events is clear looking at FAR_{LN} and RR_{LN} (Figures 2f and 2i). For instance, the average risk ratio (RR_{LN}) suggests that rainfall between 20 and 30 mm/month in the MDB region is 5.5 times more likely to occur during La Niña events compared to neutral years. The average FAR_{LN} suggests that 81% of rainfall events in this range can be attributed to La Niña events.

This risk ratio (RR_{LN}) analysis also shows a decreased risk of anomalously dry conditions, with rainfall between −5 and −15 mm/month having an average RR_{LN} is 0.59. Meaning drying of this magnitude is on average 41% less likely to occur during La Niña events than it is to occur during neutral conditions.

3.3.2. El Niño

There is a shift of the CDF to dryer values during El Niño events in the MDB region, when compared to the neutral case (Figure 2c). In terms of the significance of this shift, the neutral CDF falls outside of the El Niño CDF 95% confidence levels for the majority of rainfall anomalies, with the exception being at the extremely dry end (<−20 mm/month) of the rainfall distribution. This suggests that likelihood of having extreme dry conditions in the MDB is not significantly different in any ENSO phase.

Looking at the increased risk of moderately dry regional rainfall (−21 to −10 mm/month) during El Niño years, the mean risk ratio (RR_{EN}) suggests that this is 1.4 times more likely to occur when compared to neutral years (Figure 2i). In this situation the mean FAR_{EN} suggests that only roughly 30% of events with this magnitude can be attributed to El Niño events (Figure 2f).

On the flip side, the RR_{EN} also indicates that normal and increased rainfall is much less likely during an El Niño event. For instance, the RR_{EN} of having normal rainfall (e.g., between ± 5 mm/month) is 0.62, suggesting that normal rainfall in this region is 38% less likely to occur during El Niño events. On the other hand, anomalous rainfall increases of between 5 and 20 mm/month are approximately 62% (RR_{EN} = 0.38) less likely to occur during El Niño events than they are during neutral conditions.

4. Case Study of the September–October 2022 Rainfall Anomalies

This FAR analysis can also be used to focus in on an individual past anomalous rainfall month or season to understand the role of ENSO in driving the anomaly as is commonly done when the FAR method is applied to understand the human influence. To this end, we consider the EA region rainfall anomalies of October 2022, a La Niña year, with a rainfall anomaly in excess of 63 mm (Table 1). As this magnitude of rainfall anomaly has not occurred in the past during neutral or El Niño years, the FAR_{LN} was 1, while the Risk Ratio (RN_{LN}) was not defined. This means that a rainfall anomaly of this magnitude had not occurred in the absence of La Niña

Table 1
Table of Australian Regional Rainfall Anomalies (mm/month) and the Associated FAR_{LN} and RR_{LN} for Spring Months of 2022 During a La Niña Event

		2022 Month		
Region	Metric	September	October	November
EA	Anomaly	29.84	63.23 (highest on record)	23.01
	FAR_{LN}	0.86	1	0.82
	RR_{LN}	7.3	undefined	5.57
SEA	Anomaly	24.43	90.14 (highest on record)	47.94
	FAR_{LN}	0.44	1	1
	RR_{LN}	1.79	undefined	undefined
MDB	Anomaly	46.44	99.1 (highest on record)	31.74
	FAR_{LN}	1	1	0.94
	RR_{LN}	undefined	undefined	17.08

events in the past. In fact, an EA regional rainfall anomaly of >34 mm/month has not occurred in the absence of a La Niña event in the observational record.

The EA September and November rainfall anomalies of that same year were approximately 30 mm/month and 23 mm/month, respectively (Table 1). The September (November) FAR_{LN} was 0.86 (0.82), meaning that 86% (82%) of events of this magnitude or greater can be attributed to La Niña conditions, while the risk ratio (RR_{LN}) was 7.25 (5.56). This means that the September (November) rainfall anomalies were more than 7 (5) times more likely to occur due to the ongoing La Niña event than in an ENSO neutral phase.

5. Changes in Australian Region Rainfall Response to ENSO

The fact that the La Niña CDF (calculated from 1950 to 2022) for all regions is near and sometimes wetter than the 95% confidence interval (Figures 2a and 2c) suggests that the rainfall response to La Niña events in the recent period was wetter than it has been in the past. To further examine this, we separate the regional rainfall into two groups containing roughly even numbers (pre and post 1960) and plot it against ENSO (Nino 3.4 region SSTA) (Figure 1). This plot, along with the fitted second order polynomials shows that the rainfall response to La Niña events is more extreme (or amplified) in the post-1960 period, suggesting a possible amplifying role for anthropogenic climate change. This is supported by plotting the 95% confidence bounds generated by randomly selected 73 years of SON rainfall and ENSO data from the full 123 years record and repeating 1000 times. This confidence interval reveals that La Nina events in the most recent period are significantly wetter than those at other times in the observational record (red fitted line in Figures 1b–1d). It is also noted that neutral conditions in the earlier period appear to be drier than at other times in the observational record (blue fitted line in Figures 1b–1d).

The impact of anthropogenic climate change on the recent increases in rainfall associated with La Niña events is also supported by recent literature focusing on the rainfall associated with individual rainfall events (J. P. Evans & Boyer-Souchet, 2012; Ummenhofer et al., 2015). For instance, Evans and Boyer-Souchet (2012) along with Ummenhofer et al. (2015) investigated the role of anthropogenic warming in the extremely high east Australian rainfall that occurred during the 2010/2011 La Niña event. Both studies suggested that the observed western Pacific warming, which had previously been attributed to humans, increased the likelihood of the extreme rainfall response.

6. Discussion and Conclusions

In this study we utilized the well-known method of FAR, which is commonly used to identify the role of anthropogenic forcing in modulating the occurrence of weather and climate extremes, to quantify the role of ENSO in modulating Australian regional rainfall. We focused on the east Australian region and two additional regions that were largely contained within this region.

For all analyzed regions we find clear shifts in Cumulative Distribution Function (CDF) toward wetter conditions during La Niña events, while CDF shifts toward dryer conditions are identified for El Niño conditions. As all ENSO phase CDF distributions for a particular region typically begin at a similar anomalously dry precipitation anomaly, the CDF changes appear to be largely related to changes in the extent of the wet end of the distribution. That is, the wettest precipitation values in the La Nina CDF is typically much wetter than the wettest precipitation values during neutral or El Nino CDFs. The CDF shifts during La Niña events led to changes in the Risk Ratio (RR_{LN}) which generally have a positive slope, meaning wet conditions are more likely, while dry conditions are less likely, though the exact details differ from region to region. On the other hand, CDF shifts during El Niño events typically led to a negative slope in the Risk Ratio (RR_{EN}), meaning that dry conditions become more likely, while neutral and wet conditions become less likely. Both of these points are generally consistent with the recent work of Tozer

et al. (2023) which sought to identify how ENSO impacts the odds of average Australian rainfall being in wet or dry tercile.

Here, we extended on this earlier work by explicitly calculating the ENSO induced change in risk for all observed rainfall rates for the three eastern Australian regions, which are available in Tables S1–S3 in Supporting Information S1. As such, this study allows us to now quantify how large the change in rainfall risk is, rather than relying on more qualitative statements. We also applied this method to better understand the role of ENSO in the rainfall of SON 2022 (Table 1) to demonstrate how this method can be used for individual events.

The apparent asymmetry in ENSOs impact on Australia is clearly seen in the EA and MDB regions, where the FAR_{LN} and RR_{LN} are larger for positive rainfall anomalies than the FAR_{EN} and RR_{EN} are for negative rainfall anomalies. In contrast, the SEA region appears to display slightly larger impacts during El Nino events than La Nina events. What is also apparent is that this method still identifies statistically significant CDF changes even in the smaller regions, suggesting the method may also be applicable at even smaller spatial scales than utilised here.

We see this paper as a proof of concept for utilizing the FAR method to attribute rainfall changes over a region to a specific mode of climate variability (i.e., climate drivers). Though, we acknowledge that at some locations, like Australia, numerous modes of climate variability that impact regional rainfall can display anomalies at the same time. The separation of signals from multiple climate driver is possible, though the ideal methodological choice is still debated (e.g., Liguori et al., 2022; Risbey et al., 2009), but beyond the scope of the current manuscript.

We also identified an apparent change in the rainfall associated with La Niña events that is consistent with the impact of anthropogenic Climate Change reported in early single event studies (Ummenhofer et al., 2015). That is, the rainfall amount expected for a La Niña event of a given magnitude is higher in the most recent period (post-1960) than that seen in the earlier period (pre-1960). The effects of climate change can occur via direct changes to ENSO and its teleconnection mechanisms (Cai et al., 2021); through thermodynamical changes (C. T. Y. Chung & Power, 2016); or indirectly through localized changes like regional SST variability (van Rensch et al., 2015). Consequently, periods of extreme climate variability and climate change appear to have become inextricably linked and projections suggest that these links to be strengthened in the future (McGregor et al., 2022; Perry et al., 2017, 2020; Power & Delage, 2018).

To date, however, attribution analysis has been used to either attribute a role of climate change for a particular climate event (Lewis & Karoly, 2013; Stone & Allen, 2005; Stott et al., 2004), or to look at the role played natural variability, as in this study. Given that the combined effects from internal climate variability (which can include signals from different modes of climate variability) and climate change, which expected to become more prevalent in the future, examining attribution from a perspective that includes multiple factors is a useful area for future expansion. In epidemiological research, the discipline from which the concepts of attributable risk were developed, there are multi-factorial approaches that can be used to partition the role of different exposures to disease (Land et al., 2001). Such approaches could also be applied to determine the relative role of both modes of variability and climate change to a given event. However, it seems likely that this multifactor approach may be limited to climate model simulations due to difficulties identifying the anthropogenically forced response in the observations (Coats & Karnauskas, 2017).

Data Availability Statement

All data used in this study are publicly available. The Australian regional average rainfall for SON was sourced from the Bureau of Meteorology's Australian Gridded Climate Data (AGCD) for the period 1900–2022 (http://www.bom.gov.au/cgi-bin/climate/change/timeseries.cgi). ERSST v5 data set used for the calculation of Nino 3.4 region SSTA are available (Huang et al., 2017).

Acknowledgments
All authors would like to acknowledge funding support from the Australian Government under the National Environmental Science Program. Open access publishing facilitated by Monash University, as part of the Wiley - Monash University agreement via the Council of Australian University Librarians.

References

Allen, M. (2003). Liability for climate change. *Nature*, *421*(6926), 891–892. https://doi.org/10.1038/421891a

Cai, W., Santoso, A., Collins, M., Dewitte, B., Karamperidou, C., Kug, J.-S., et al. (2021). Changing El Niño–Southern Oscillation in a warming climate. *Nature Reviews Earth & Environment*, *2*(9), 628–644. https://doi.org/10.1038/s43017-021-00199-z

Cai, W., van Rensch, P., Cowan, T., & Sullivan, A. (2010). Asymmetry in ENSO teleconnection with regional rainfall, its Multidecadal variability, and impact. *Journal of Climate*, *23*(18), 4944–4955. https://doi.org/10.1175/2010JCLI3501.1

Chiew, F. H. S., Piechota, T. C., Dracup, J. A., & McMahon, T. A. (1998). El Nino/Southern Oscillation and Australian rainfall, streamflow and drought: Links and potential for forecasting. *Journal of Hydrology*, *204*(1), 138–149. https://doi.org/10.1016/S0022-1694(97)00121-2

Chung, C., Boschat, G., Taschetto, A., Narsey, S., McGregor, S., Santoso, A., & Delage, F. (2023). Evaluation of seasonal teleconnections to remote drivers of Australian rainfall in CMIP5 and CMIP6 models. *Journal of Southern Hemisphere Earth Systems Science*, *73*(3), 219–261. https://doi.org/10.1071/es23002

Chung, C. T. Y., & Power, S. B. (2016). Modelled impact of global warming on ENSO-driven precipitation changes in the tropical Pacific. *Climate Dynamics*, *47*(3), 1303–1323. https://doi.org/10.1007/s00382-015-2902-9

Coats, S., & Karnauskas, K. B. (2017). Are simulated and observed twentieth century tropical Pacific Sea surface temperature trends significant relative to internal variability? *Geophysical Research Letters*, *44*(19), 9928–9937. https://doi.org/10.1002/2017GL074622

Evans, A., Jones, D., Smalley, R., & Lellyett, S. (2020). An enhanced gridded rainfall analysis scheme for Australia. In *Bureau research report* (Vol. 41, p. 45). Australian Bureau of Meteorology.

Evans, J. P., & Boyer-Souchet, I. (2012). Local sea surface temperatures add to extreme precipitation in northeast Australia during La Niña. *Geophysical Research Letters*, *39*(10). https://doi.org/10.1029/2012GL052014

Hendon, H. H., Lim, E.-P., Arblaster, J. M., & Anderson, D. L. T. (2014). Causes and predictability of the record wet east Australian spring 2010. *Climate Dynamics*, *42*(5), 1155–1174. https://doi.org/10.1007/s00382-013-1700-5

Hope, P., Lim, E.-P., Hendon, H., & Wang, G. (2018). The effect of increasing CO_2 on the extreme September 2016 rainfall across Southeastern Australia. *Bulletin of the American Meteorological Society*, *99*(1), S133–S138. https://doi.org/10.1175/BAMS-D-17-0094.1

Huang, B., Thorne, P. W., Banzon, V. F., Boyer, T., Chepurin, G., Lawrimore, J. H., et al. (2017). Extended reconstructed sea surface temperature, version 5 (ERSSTv5): Upgrades, validations, and intercomparisons. *Journal of Climate*, *30*(20), 8179–8205. https://doi.org/10.1175/jcli-d-16-0836.1

Karoly, D. J., Black, M. T., King, A. D., & Grose, M. R. (2016). The roles of climate change and El Niño in the record low rainfall in October 2015 in Tasmania, Australia. *Bulletin of the American Meteorological Society*, *97*(12), S127–S130. https://doi.org/10.1175/BAMS-D-16-0139.1

Kiem, A. S., Franks, S. W., & Kuczera, G. (2003). Multi-decadal variability of flood risk. *Geophysical Research Letters*, *30*(2), 1035. https://doi.org/10.1029/2002GL015992

King, A. D. (2018). Natural variability not climate change drove the record wet winter in southeast Australia. *Bulletin of the American Meteorological Society*, *99*(1), S139–S143. https://doi.org/10.1175/BAMS-D-17-0087.1

King, A. D., Alexander, L. V., & Donat, M. G. (2013). Asymmetry in the response of eastern Australia extreme rainfall to low-frequency Pacific variability. *Geophysical Research Letters*, *40*(10), 2271–2277. https://doi.org/10.1002/grl.50427

King, A. D., Black, M. T., Min, S.-K., Fischer, E. M., Mitchell, D. M., Harrington, L. J., & Perkins-Kirkpatrick, S. E. (2016). Emergence of heat extremes attributable to anthropogenic influences. *Geophysical Research Letters*, *43*(7), 3438–3443. https://doi.org/10.1002/2015GL067448

Land, M., Vogel, C., & Gefeller, O. (2001). Partitioning methods for multifactorial risk attribution. *Statistical Methods in Medical Research*, *10*(3), 217–230. https://doi.org/10.1177/096228020101000304

Lewis, S. C., & Karoly, D. J. (2013). Anthropogenic contributions to Australia's record summer temperatures of 2013. *Geophysical Research Letters*, *40*(14), 3705–3709. https://doi.org/10.1002/grl.50673

Liguori, G., McGregor, S., Singh, M., Arblaster, J., & Di Lorenzo, E. (2022). Revisiting ENSO and IOD contributions to Australian precipitation. *Geophysical Research Letters*, *49*(1), e2021GL094295. https://doi.org/10.1029/2021GL094295

McBride, J. L., & Nicholls, N. (1983). Seasonal relationships between Australian rainfall and the Southern Oscillation. *Monthly Weather Review*, *111*(10), 1998–2004. https://doi.org/10.1175/1520-0493(1983)111<1998:SRBARA>2.0.CO;2

McGregor, S., Cassou, C., Kosaka, Y., & Phillips, A. S. (2022). Projected ENSO teleconnection changes in CMIP6. *Geophysical Research Letters*, *49*(11), e2021GL097511. https://doi.org/10.1029/2021GL097511

Nicholls, N. (1988). More on early ENSOs: Evidence from Australian documentary sources. *Bulletin of the American Meteorological Society*, *69*(1), 4–6. https://doi.org/10.1175/1520-0477(1988)069<0004:MOEEEF>2.0.CO;2

Nicholls, N. (1997). Increased Australian wheat yield due to recent climate trends. *Nature*, *387*(6632), 484–485. https://doi.org/10.1038/387484a0

Perry, S. J., McGregor, S., Gupta, A. S., & England, M. H. (2017). Future changes to El Niño–Southern Oscillation temperature and precipitation teleconnections. *Geophysical Research Letters*, *44*(20). https://doi.org/10.1002/2017GL074509

Perry, S. J., McGregor, S., Gupta, A. S., England, M. H., & Maher, N. (2020). Projected late 21st century changes to the regional impacts of the El Niño-Southern Oscillation. *Climate Dynamics*, 1–18.

Planton, Y. Y., Guilyardi, E., Wittenberg, A. T., Lee, J., Gleckler, P. J., Bayr, T., et al. (2020). Evaluating climate models with the CLIVAR 2020 ENSO metrics package. *Bulletin of the American Meteorological Society*, *102*(2), 1–57. https://doi.org/10.1175/BAMS-D-19-0337.1

Power, S. B., Casey, T., Folland, C., Colman, A., & Mehta, V. (1999). Inter-decadal modulation of the impact of ENSO on Australia. *Climate Dynamics*, *15*(5), 319–324. https://doi.org/10.1007/s003820050284

Power, S. B., & Colman, R. (2006). Multi-year predictability in a coupled general circulation model. *Climate Dynamics*, *26*(2–3), 247–272. https://doi.org/10.1007/s00382-005-0055-y

Power, S. B., & Delage, F. P. D. (2018). El Niño-Southern oscillation and associated climatic conditions around the world during the latter half of the twenty-first century. *Journal of Climate*, *31*(15), 6189–6207. https://doi.org/10.1175/JCLI-D-18-0138.1

Power, S. B., Haylock, M., Colman, R., & Wang, X. (2006). The predictability of interdecadal changes in ENSO activity and ENSO teleconnections. *Journal of Climate*, *19*(19), 4755–4771. https://doi.org/10.1175/JCLI3868.1

Risbey, J. S., Pook, M. J., McIntosh, P. C., Wheeler, M. C., & Hendon, H. H. (2009). On the remote drivers of rainfall variability in Australia. *Monthly Weather Review*, *137*(10), 3233–3253. https://doi.org/10.1175/2009MWR2861.1

Stone, D. A., & Allen, M. R. (2005). The end-to-end attribution problem: From emissions to impacts. *Climatic Change*, *71*(3), 303–318. https://doi.org/10.1007/s10584-005-6778-2

Stott, P. A., Stone, D. A., & Allen, M. R. (2004). Human contribution to the European heatwave of 2003. *Nature*, *432*(7017), 610–614. https://doi.org/10.1038/nature03089

Taschetto, A. S., Ummenhofer, C. C., Stuecker, M. F., Dommenget, D., Ashok, K., Rodrigues, R. R., & Yeh, S.-W. (2020). ENSO atmospheric teleconnections. In M. J. McPhaden, A. Santoso, & W. Cai (Eds.), *El Niño Southern Oscillation in a changing climate* (p. 26). American Geophysical Union.

Timmermann, A., An, S.-I., Kug, J.-S., Jin, F.-F., Cai, W., Capotondi, A., et al. (2018). El Niño–Southern Oscillation complexity. *Nature*, *559*, 535–545. https://doi.org/10.1038/s41586-018-0252-6

Tozer, C. R., Risbey, J. S., Monselesan, D. P., Pook, M. J., Irving, D., Ramesh, N., et al. (2023). Impacts of ENSO on Australian rainfall: What not to expect. *Journal of Southern Hemisphere Earth Systems Science*, *73*(1), 77–81. https://doi.org/10.1071/ES22034

Ummenhofer, C. C., Sen Gupta, A., England, M. H., Taschetto, A. S., Briggs, P. R., & Raupach, M. R. (2015). How did ocean warming affect Australian rainfall extremes during the 2010/2011 La Niña event? *Geophysical Research Letters*, *42*(22), 9942–9951. https://doi.org/10.1002/2015GL065948

Van Dijk, A. I. J. M., Beck, H. E., Crosbie, R. S., De Jeu, R. A. M., Liu, Y. Y., Podger, G. M., et al. (2013). The Millennium Drought in southeast Australia (2001-2009): Natural and human causes and implications for water resources, ecosystems, economy, and society. *Water Resources Research*, *49*(2), 1040–1057. https://doi.org/10.1002/wrcr.20123

van Rensch, P., Gallant, A. J. E., Cai, W., & Nicholls, N. (2015). Evidence of local sea surface temperatures overriding the southeast Australian rainfall response to the 1997–1998 El Niño. *Geophysical Research Letters*, *42*(21), 9449–9456. https://doi.org/10.1002/2015GL066319